Precipitation Structure of the Cloud Clusters in a Tropical Easterly Wave

COLLEEN A. LEARY

Atmospheric Science Group, Texas Tech University, Lubbock, TX 79409

(Manuscript received 3 June 1983, in final form 4 October 1983)

ABSTRACT

This paper describes the statistics of precipitation observed over the 42.5×10^4 km^2 area covered by all four of the GATE digitized radars for the period 2300 GMT 4 September 1974 to 2400 GMT 5 September 1974. The period coincided with the GATE double cloud cluster of 5 September, the latter stages in the life cycle of the squall line system of 4–5 September and the passage of the trough of an easterly wave in the midtropospheric flow. Hourly precipitation amounts over 4 km × 4 km data bins were stratified by time, data source, individual mesoscale precipitation feature (1 of 12), type of precipitation (convective or stratiform) and, if convective, cell top height. Each subtotal contained a total precipitation amount and the number of 4 km × 4 km bins which contributed to the total. From these subtotals a variety of precipitation statistics were compiled.

The precipitation statistics of the 5 September double cloud cluster confirm the importance of deep convection in producing observed tropical mesoscale precipitation patterns. They also underscore the importance of stratiform precipitation in non-squall cloud clusters as well as in squall line systems. The evolution of the total, convective and stratiform amounts of rainfall in the 5 September double cloud cluster is similar to that of the mesoscale precipitation features of which it is composed and also to the evolution of squall line systems consisting of a single intense mesoscale precipitation feature. The time lag in the development of stratiform precipitation suggests that storage of water condensed in convective cells after transfer to the anvil may be an important component of the water budget of a mesoscale precipitation feature. When precipitation from the 4–5 September squall line system and the 5 September double cloud cluster are combined to show the evolution of precipitation over the large mesoscale in and near the trough of the easterly wave, the total rainfall is nearly constant for over 24 hours. This result is consistent with the statistical quasi-equilibrium assumption Arakawa and Schubert used to provide a closed parameterization of cumulus convection for use in prognostic models of large-scale atmospheric motion.

1. Introduction

One important result of the Global Atmospheric Research Program's Atlantic Tropical Experiment (GATE) has been the recognition that the precipitation patterns associated with tropical cloud clusters display mesoscale structure, with both convective precipitation from cumulonimbus cells (~2–20 km in horizontal scale) of different heights and stratiform precipitation over larger areas (~10^4 km^2) where vertical air motions are much weaker. Although mesoscale structure and areas of widespread lighter precipitation had been noted earlier (Hamilton and Archbold, 1945; Zipser, 1969), the data collected during GATE, when four digitized radars covered an area of 42.5×10^4 km^2 over the eastern North Atlantic Ocean, have made possible the first quantitative estimates of the precipitation from tropical cloud clusters (a detailed review is presented by Houze and Betts, 1981).

Cheng and Houze (1979) determined the distribution of total rain among echoes of various sizes and types for the entire period of GATE. For their sample they chose the radar echoes observed on board the U.S. NOAA ship *Oceanographer* each day during GATE at 1200 GMT (Houze and Cheng, 1977). They derived quantitative precipitation intensities from the radar data and followed the life history of each echo to determine the heights of cell tops. They found that 43% of the precipitation in their sample fell in areas of widespread stratiform rain.

Houze (1977) noted that the widespread stratiform rain accounted for 40% of the total rainfall in the 4–5 September 1974 tropical squall-line system observed over the GATE data network. In other studies of individual GATE squall-line systems, Gamache and Houze (1983) found that 49% of the rain was stratiform for the 12 September case, and Houze and Rappaport (1984) found that 42% of the rain was stratiform for the 28 June case. Zipser *et al.* (1981), in a detailed case study of a mesoscale convective band observed over the GATE network on 14 September 1974, found that, for a portion of its lifetime, 50–55% of the rainfall it produced fell in areas of stratiform precipitation.

This paper describes precipitation statistics obtained from the data collected by all four GATE radars for the period 2300 (all times are GMT) 4 September to 2400 5 September 1974. This period was chosen to coincide with the life cycle of the double cloud cluster which passed through the GATE data network on 5 September. The structure and evolution of this cloud

cluster have already been studied in some detail (Leary, 1979; Leary and Houze, 1979a). This double cloud cluster is of particular interest for two reasons. First, it contained several mesoscale precipitation features of horizontal scale ~ 50–200 km, possessing both convective and stratiform precipitation during their life cycles. One of these features was the squall line system studied by Houze (1977) in the latter stages of its life cycle. Second, the double cloud cluster, together with the 4–5 September squall-line system, accounted for virtually all of the rainfall associated with the region just ahead of and in the trough of a midtropospheric synoptic-scale easterly wave. The occurrence of cloud clusters over the area observed by the GATE radars (see Fig. 1) was modulated by the passage of such waves with a 3–4 day period (Payne and McGarry, 1977). A maximum of cloudiness associated with cloud clusters occurred at and ahead of the trough axes of the easterly waves, with a minimum at and ahead of the ridge axes. Hudlow (1979) observed the same relationship between the waves and radar-derived precipitation amounts.

This paper aims to describe the precipitation statistics of the cloud clusters in the trough of a tropical easterly wave in a manner compatible with understanding the life cycles of the cloud clusters, their water budget and the relationship of the cloud clusters to their constituent mesoscale precipitation features, which contain convective cells of different heights and widespread stratiform rain.

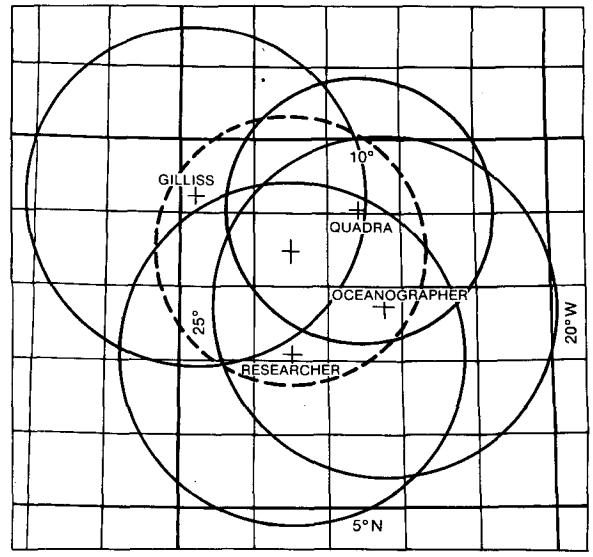

FIG. 1. Crosses mark the positions of the four digitized GATE radars on 5 September 1974 and the solid circles show their overlapping coverage. The fifth cross and the dashed circle mark the center and the outer limits of the central array for which Hudlow (1977) computed hourly rainfall amounts. Each square is 1° by 1°.

2. Data

Four shipboard C-band radars were used to collect quantitative data during GATE. Fig. 1 shows their overlapping coverage. Hudlow *et al.* (1979) have described in detail the characteristics of these radar systems, as well as their calibrations and intercomparisons with each other and with raingage data to determine rainfall rates and amounts. The success of the calibrations and intercomparisons of the radars made it possible to produce hourly rainfall accumulations (Hudlow, 1977, 1979; Hudlow and Patterson, 1979) for 4 km × 4 km data bins over an area with a radius of 204 km from the center of the GATE data network (dashed circle in Fig. 1).

Their hourly accumulations were derived by trapezoidal integrations of five low-level (hybrid) reflectivity scans which were normally available every 15 minutes in Cartesian coordinates from the four radars after extensive preliminary data processing. For each hour ending at time T, the scans at T, $T - 15$ min, $T - 30$, $T - 45$ and $T - 60$ min were used for the integration, with weighting factors of 0.125, 0.25, 0.25, 0.25 and 0.125 respectively. Rainfall amounts associated with each scan were calculated using the relationship

$$Z = 230R^{1.25}, \quad (1)$$

derived using GATE radar and raingage data (Hudlow *et al.*, 1979), where Z is the radar reflectivity factor in $mm^6\ m^{-3}$ and R is the rainfall rate in $mm\ h^{-1}$. Corrections to the Cartesian array of reflectivity values archived for each of the four radars for attenuation due to atmospheric gases and biases determined by intercomparisons and calibrations (Hudlow *et al.*, 1979) were incorporated into the hourly rainfall calculations.

For Phase III of GATE (30 August–19 September), during which the 5 September double cloud cluster passed through the GATE data network, the hourly rainfall amounts for the central array were obtained by merging rainfall amounts derived from all four quantitative radars. The merging process consisted of averaging nonzero rainfall amounts from the various radars for the common data bins inside the central array (Hudlow and Patterson, 1979). The determination of the precipitation statistics for the 5 September cloud cluster relied principally upon these hourly rainfall accumulations for the central array (Hudlow, 1977).

The mesoscale precipitation features in the 5 September double cloud cluster in many cases extended beyond the central array of hourly precipitation values. In such cases, and for the hour from 2200 to 2300, when no hourly precipitation amounts were available from the central array, hourly precipitation amounts were supplemented using data from the individual radars. Where the coverage of two or more radars overlapped, proximity to the precipitation and amount of intervening precipitation determined the choice of which radar's data were most representative.

The hourly precipitation amounts for the individual radars outside the central array were calculated using the archived Cartesian datasets for each radar (Hudlow, 1976a,b; P. M. Austin, 1976a; G. L. Austin, 1977a). For each hour, the trapezoidal integration scheme described above, the bias and attenuation corrections of Hudlow *et al.* (1979) and the Z–R relationship (1) were applied to the Cartesian datasets for each radar in order to make the hourly precipitation amounts from the individual radars comparable to the values for the central array. The mean position of each ship during 5 September, obtained by averaging hourly values of ship position was rounded to the position of the closest intersection of four bins. In this way, the 26 536 4 km $\times$ 4 km squares of the four ships and the central array overlapped and every bin could be unambiguously identified with one or more of the four radars and the central array. When scans were missing for the individual radars, hourly rainfall estimates were obtained by adding the weighting factors of the missing scans to that of the scan or scans in the 1-hour sequence closest in time to the missing scan or scans. For example, if the scan at time T were missing, the scan at $T - 15$ min was assigned a weight of 0.375.

The archived Cartesian datasets for each radar also proved useful in defining the boundaries of the mesoscale precipitation features for the hourly precipitation maps. Other forms of the GATE radar data made it possible to distinguish between convective and stratiform precipitation and to determine echo top heights, as described in more detail in Section 3. These included movie films of the radar scopes (Hudlow, 1975a, 1976c; G. L. Austin, 1977b; P. M. Austin, 1976b) and vertical cross sections (Leary and Houze, 1979a,b) constructed using the raw digital data (Hudlow, 1975b; P. M. Austin, 1976c; G. L. Austin, 1977b). Echo top heights could be obtained directly from the vertical cross sections. For the three radars for which radar films at a sequence of tilt angles were available [the Sperry SP6504 missile-tracking radar on board *Quadra* and the National Oceanic and Atmospheric Administration (NOAA) radars on board *Oceanographer* and *Researcher*], echo top charts were constructed by tracing PPI (Plan Position Indicator) displays for each tilt angle of a given scan on the same chart. Using relationships between tilt angle and range, it was possible to label these charts with echo top heights for each echo. These echo top height charts were constructed for each scan during the time period of interest.

3. Methods of analysis

a. Categorization of the precipitation by mesoscale feature

Leary and Houze (1979a), in a detailed descriptive study of the structure and evolution of the 5 September cloud cluster, identified six mesoscale features which made up the precipitation pattern. Their analysis was based on examination of vertical cross sections and single tilt angle radar reflectivity data and time continuity. With the slight differences discussed below, this paper uses the same nomenclature. Fig. 2 illustrates schematically, for four different time periods, the twelve precipitation features identified for categorization. This figure is an adaptation of Fig. 4 from Leary and Houze (1979a).

Each 4 km $\times$ 4 km square with a nonzero hourly precipitation value was assigned to one of the precipitation features. When interactions among the individual features made delineating their boundaries difficult, time continuity was applied to make decisions. The following subsections describe briefly the twelve precipitation features and their contributions to the total amount of precipitation observed over the data collection network shown in Fig. 1 for the time period from 2300 on 4 September to 2400 on 5 September.

1) THE SQUALL LINE SYSTEM OF 4–5 SEPTEMBER (SQA AND SQB)

Nearly 20% (see Fig. 3) of the total amount of rain which fell over the area covered by the four radars during the 25 h period was associated with a squall line system which had developed and reached its maximum intensity on 4 September. Houze (1977) studied this system in great detail, identifying it as a mesoscale precipitation feature distinctive for its large size, great intensity as measured by high rainfall rates, deep convection and long lifetime of 24 hours. For the first eight hours of the 25 h period described in this paper, the squall line system was present in the latter stages of its life cycle. For this study, the precipitation which fell in the squall line system during the time period of interest was divided into two features, denoted SQA and SQB. Leary and Houze (1979a) identified both SQA and SQB, but counted them as a single mesoscale precipitation feature. Feature SQA, which contained 86% of the precipitation in the squall line system during the 25-h period, was clearly distinct from the precipitation features in the cloud cluster of 5 September. Feature SQB, on the other hand, denotes a portion of the squall line system that became detached from the system (Fig. 2a), moved towards the northeast (while SQA moved to the west) and by 1100 (Fig. 2b) on 5 September, became completely incorporated into the 5 September cloud cluster. In this and later sections of this paper, statistics computed *including squall line* comprise precipitation from both SQA and SQB. Statistics for the *cloud cluster only* include SQB, but not SQA. Since SQB accounted for less than 3% of the rainfall during the 25 h period, the decision to include it in both samples because it formed a part of both the squall line system and the cloud cluster did not greatly influence the outcome of the statistical calculations.

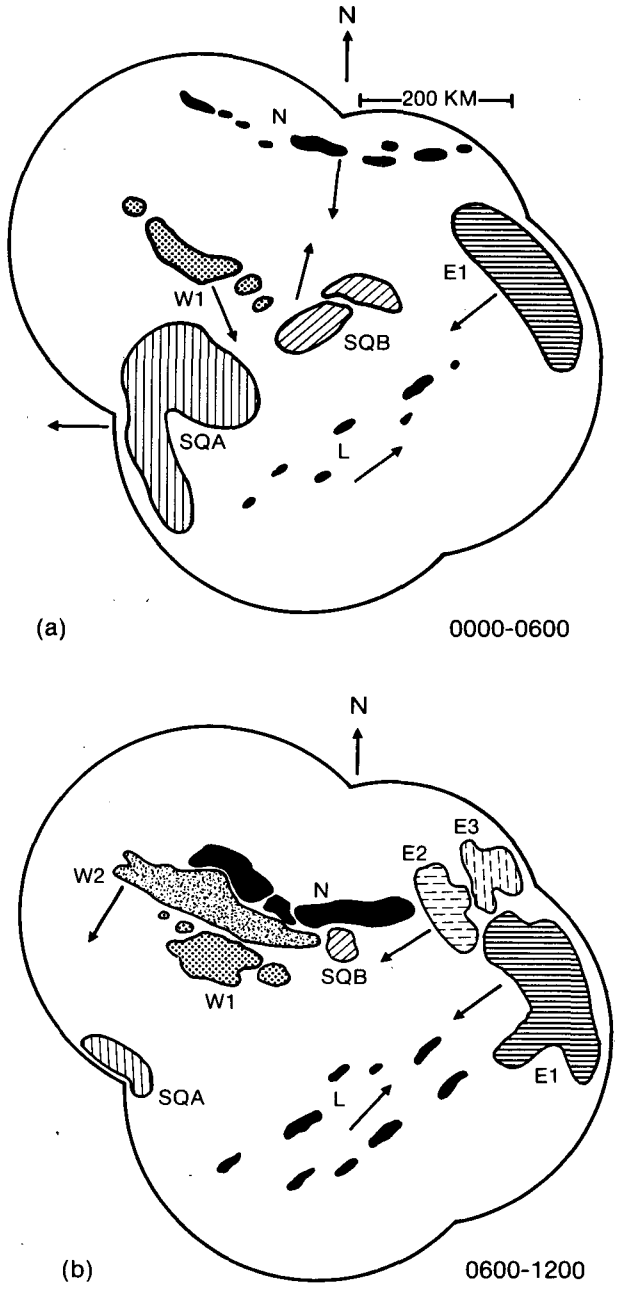

FIG. 2. Schematic illustration of the precipitation features as observed using data from the four GATE radars on 5 September 1974. Arrows denote the direction of motion of the features when it could be determined. Four panels show the features during the GMT time periods (a) 0000–0600, (b) 0600–1200, (c) 1200–1800 and (d) 1800–2400. Outer boundary as in Fig. 1. Shading differentiates the precipitation features.

2) THE EASTERN PORTION OF THE CLOUD CLUSTER (E1, E2, E3, E2 + E3)

At 1200 on 5 September, the precipitation pattern of the cloud cluster had a distinctive double structure (Fig. 1 of Leary, 1979). The precipitation features making up the eastern portion (see Fig. 2) of the cloud cluster accounted for 27% of the total precipitation in the 25 h period. Of this rainfall, 68% (i.e., 18% of total rain) fell from Feature E1. Features E2 and E3 formed to the north of E1. After 1400, E2 and E3 could not be distinguished from one another and the nomenclature E2 + E3 was used to describe the precipitation attributed jointly to them. Together E2, E3 and E2 + E3 accounted for nearly 9% of the total precipitation in the 25 h period. Leary and Houze (1979a) recognized

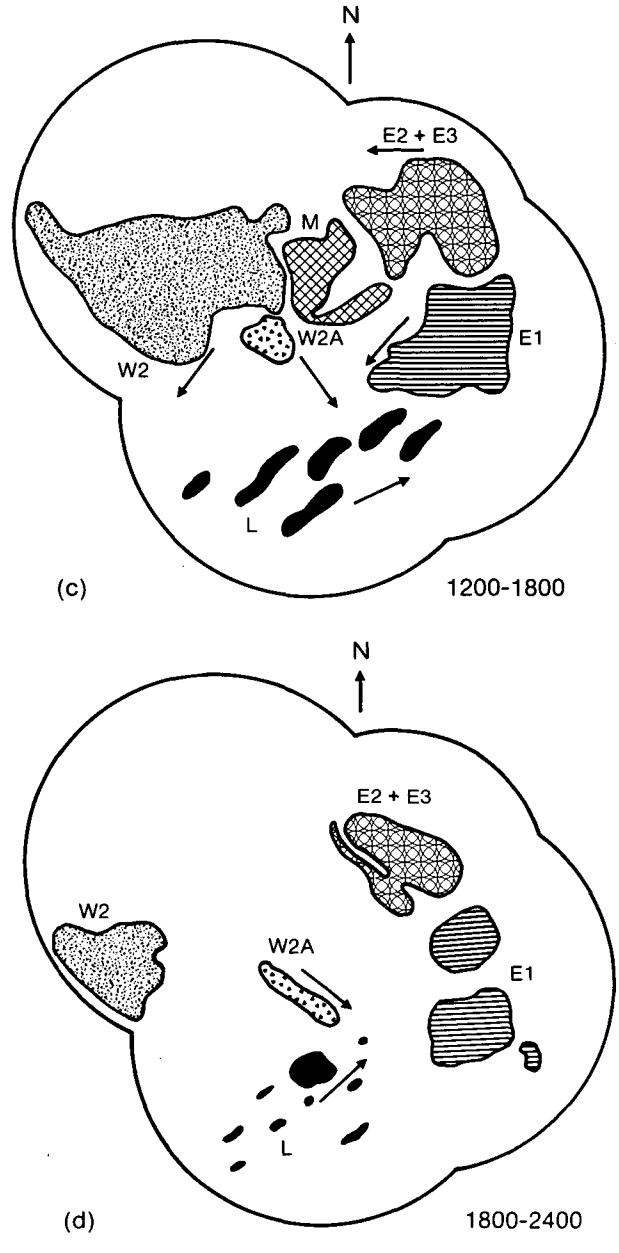

FIG. 2. (*Continued*)

E1 and E2 as separate mesoscale precipitation features. They did not distinguish E3 from E2, nor did they use the nomenclature "E2 + E3."

3) THE LONG THIN LINE OF PRECIPITATION TO THE NORTH (N)

A distinctive feature of the 5 September cloud cluster was a narrow synoptic-scale line of confluence in the low-level wind field marked by a line of cumulus clouds in the visible satellite imagery (Fig. 1 of Leary, 1979). Over the area covered by the four radars, precipitation associated with this feature is denoted by N. It moved southward during 5 September (see Fig. 2) and by 1300 could not be distinguished from the other mesoscale features of the cloud cluster, with which it interacted. While Feature N accounted for only 7% of the total rain observed during the 25 h period (Fig. 3), the mesoscale features E2, E3, and W2 (described below) all formed along it.

4) THE WESTERN PORTION OF THE CLOUD CLUSTER (W1, W2 AND W2A)

Two mesoscale features (W1 and W2) made up the western portion of the double cloud cluster of 5 Sep-

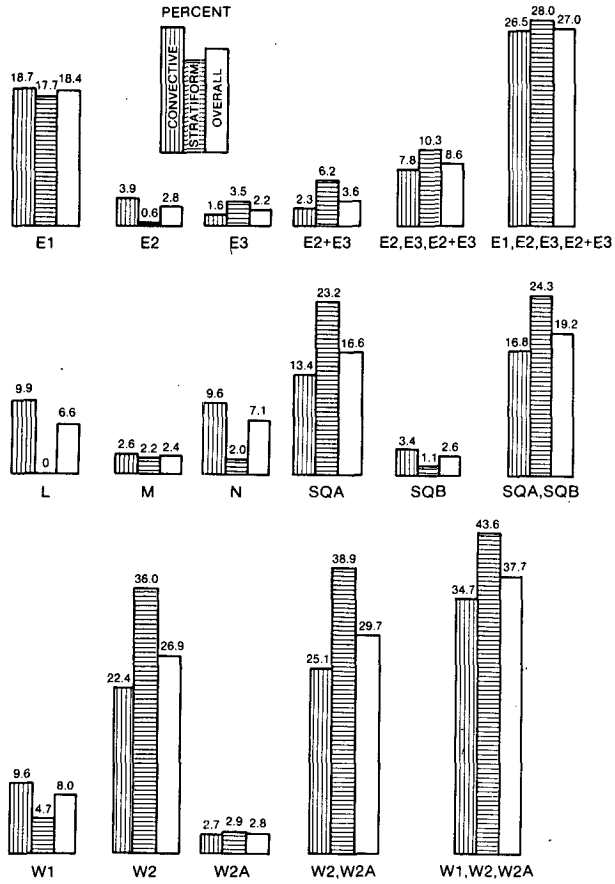

FIG. 3. Percentage contributions of individual precipitation features and combinations of precipitation features to the total amount of convective rain (vertically shaded bars), the total amount of stratiform rain (horizontally shaded bars) and the total amount of rain (unshaded bars) observed over the data collecting network in Fig. 1 during the time period 2300 4 September to 2400 5 September 1974. For comparison, the following are percentage contributions of convective rain to each of the individual precipitation features and combinations of precipitation features: E1, 68.6; E2, 93.6; E3, 48.6; E2 + E3, 42.8; E2, E3, E2 + E3, 60.9; E1, E2, E3, E2 + E3, 66.1; L, 100; M, 70.8; N, 90.9; SQA, 54.2; SQB, 86.7; SQA, SQB, 58.7; W1, 80.7; W2, 56.1; W2A, 66.2; W2, W2A, 57.0; W1, W2, W2A, 62.1.

tember. Feature W1 accounted for 8% of the total precipitation which fell in the 25 h period, while the longer-lived and much larger Feature W2 accounted for nearly 27% of the total rain. Feature W2A was a much smaller precipitation feature (slightly less than 3% of the total precipitation), originally part of W2, which separated from the larger feature and then moved (see Fig. 2) to the southeast. Leary and Houze (1979a) described W1, W2 and W2A, but counted only W1 and W2 as mesoscale precipitation features.

5) ISOLATED CONVECTIVE ECHOES (L)

In the southwestern portion of the area covered by the four radars, isolated convective radar echoes aligned in bands oriented from southwest to northeast were present for much of 5 September (see Fig. 2). They moved towards the northeast with the low-level wind flow. Their contribution to the total precipitation for the 25-hour period was 7%. Although the echoes comprising Feature L did not constitute a distinct mesoscale feature like E1 for example, they were included in the precipitation statistics for the cloud cluster because of their proximity to the features and their interaction with Feature E1, with which many of the echoes merged. Leary and Houze (1979a) identified these echoes, but did not count them as a mesoscale precipitation feature.

6) PRECIPITATION BETWEEN THE EASTERN AND WESTERN PORTIONS OF THE CLOUD CLUSTER (M)

For a period of several hours (1100–1500), a precipitation feature occurred which was not easily identified with either the eastern or western portions of the cloud cluster. Denoted M, it accounted for less than 3% of the total precipitation for the 25 h period. Leary and Houze (1979a) did not identify Feature M.

b. Categorization of precipitation as convective or stratiform

After the hourly precipitation amounts for each 4 km × 4 km square had been assigned to a particular mesoscale precipitation feature, the next step in partitioning the precipitation was to separate the precipitation into convective and stratiform components. Hourly rainfall in each 4 km × 4 km bin was assumed to be either entirely convective or entirely stratiform. The smallest ($\leq$100 km^2) precipitation areas could unambiguously be identified as the result of convective activity. Convective cells are characterized (Cheng and Houze, 1979) by high radar reflectivities, sharp horizontal gradients in reflectivity and frequent overshooting echo tops. Rapid changes (15 min to 1 h) of a factor of 5 or more in precipitation rates also indicate convective precipitation.

Precipitation areas larger than 100 km^2 frequently contain regions of stratiform precipitation, sometimes accompanied by convective cells. As noted by Cheng and Houze (1979), some subjectivity is involved in defining boundaries in these cases. Stratiform precipitation is characterized by lower reflectivities, weaker horizontal gradients of reflectivity and more uniform echo top heights than convective precipitation. The presence of a radar bright band (Leary and Houze, 1979a,b) in vertical cross sections of radar reflectivity is another factor used to identify an area as stratiform. Radar bright bands and weak horizontal gradients of radar reflectivity characterize not only widespread areas of stratiform precipitation, but also the last stage in the life cycle of an individual cumulonimbus cell (Houze, 1981). In this paper, the designation stratiform is reserved for widespread areas where the stratiform precipitation process described by Houze (1981) occurs.

For example, while dying cells in Feature L contained light rain with a noncellular appearance, none of the rain in this feature fell in a widespread area beneath an anvil cloud of mesoscale extent, so none of L's precipitation was considered stratiform. Slowly varying precipitation rates over periods of about an hour or more were also suggestive of stratiform rain. In practice, the boundary between cellular and noncellular rainfall frequently occurred along a local minimum in the hourly precipitation pattern.

While the hourly precipitation data provided some of the information necessary to discriminate between convective and stratiform precipitation, an examination of PPIs at 15-minute intervals and vertical cross sections for at least one radar was used to make a determination.

c. *Categorization of convective rain by cell top height*

All the convective rain was further subdivided by the height of the cell in which it was condensed. Each 4 km × 4 km square of hourly precipitation, if convective, was assigned to a particular cell top height. For the hour ending at time T, echo tops were examined from time $T - 90$ min to $T + 30$ min. The highest value of echo top height over this period for echoes in the vicinity ($\leqslant$30 km) of the square, using the minimum detectable signal as a threshold, was chosen for the echo top category to which the precipitation was assigned.

Echo top heights at 15-minute intervals were determined using the echo top height charts described in Section 2 and vertical cross sections (RHIs) of the digitized radar data. Echo top heights were assigned with a resolution of 1 km, although the uncertainty in estimating echo top heights is 1–3 km, with the larger uncertainty at distances greater than 150 km from the radar.

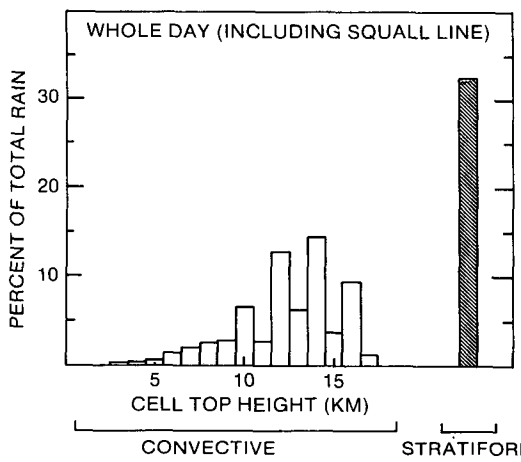

FIG. 4. Percent contributed by stratiform rain and convective cells of different heights to the total amount of rain observed over the data collecting network in Fig. 1 during the interval 2300 4 September to 2400 5 September 1974. Rainfall from all 12 precipitation features is included.

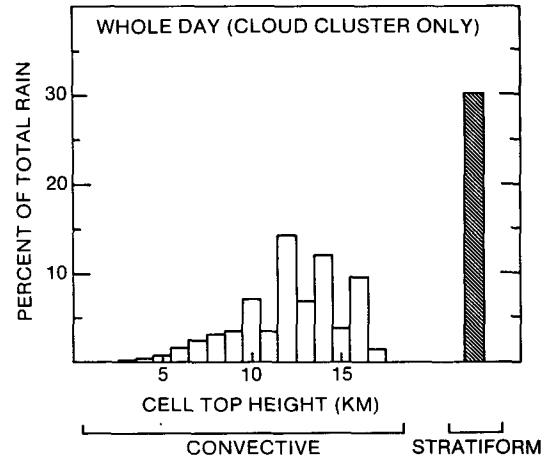

FIG. 5. As in Fig. 4, but with rain from Feature SQA excluded from the total amount of rain and the individual contributions from the stratiform and convective cell top height categories.

d. *Compilation of subtotals*

After each hourly rainfall pattern for each radar and the central array was subdivided first by mesoscale feature, then by type (convective or stratiform), then by cell top height for the convective rain and the most appropriate radar was chosen for areas outside the central array, the counting began. For the 25 h period, 1008 subtotals were tabulated. Each subtotal consisted of a label by hour, a total hourly precipitation amount, a total area with nonzero precipitation contributing to the rainfall total, a source (one of the four radars or the central array), a type (convective or stratiform) and, if convective, a cell top height. All the statistics presented in Figs. 3–17 were obtained from computations using these subtotals.

4. Results

a. *Relative amounts of stratiform rain and rain from convective cells of different heights*

Stratification of the rain for the entire 25 h period by type (stratiform and convective) and by cell top height for convective rain produced the distributions of rainfall illustrated by Figs. 4 and 5. There is little variation in the results of the summations when all the rainfall is included (Fig. 4) and when Feature SQA, that part of the squall line system that was separate from the cloud cluster, is excluded (Fig. 5). The slightly larger fraction of stratiform rain when feature SQA is included (33% compared to 30%) is probably due to SQA being in the latter stages of its life cycle during the 25 h period, with a particularly well-developed stratiform region of precipitation (see Section 4c).

The relative proportions of convective and stratiform rain in Figs. 4 and 5 are in good agreement with the results of Cheng and Houze (1979), who used data from one radar for every day during GATE at 1200

GMT. They found that 35% of the rain observed during Phase III (of which 5 September formed a part) was stratiform. This close agreement has three implications. First, it helps justify the statistical approach defined by Houze and Cheng (1977) and applied by Cheng and Houze (1979) to obtain precipitation estimates over a lengthy period of time. Second, it suggests that the precipitation patterns observed over the GATE network on 5 September were not fundamentally different from the other major precipitation events observed during GATE, thus providing some grounds for generalizing the results of this section. Third, the agreement lends confidence that the partially subjective methods described in Section 3 to distinguish convective and stratiform precipitation are consistent with the similar (and also partly subjective) method used by Cheng and Houze (1979).

Uncertainties in the estimation of cell top heights are evident in both Figs. 4 and 5, particularly for the deeper cells, where there is a distinct bias towards identifying cells with even top heights. The cumulative frequency distributions of convective rainfall shown in Fig. 6 (all features) and Fig. 7 (excluding Feature SQA) suppress this bias and show more clearly the importance of deep cells in producing convective rainfall. Cheng and Houze (1979) noted for their statistical sample that overall and for each of the three phases of GATE a preponderance of the total convective rain fell from cells with tops at or in excess of 7 km. That conclusion is borne out in this detailed study of all the rainfall observed on one particular day, 5 September. Only 5% of the total rainfall could be attributed to cells with tops of 7 km or below, even less than that observed by Cheng and Houze (1979). This result underscores the importance of deep tropical convection noted much earlier by Riehl and Malkus (1958). The cumulative distributions in Figs. 6 and 7 show little variation with inclusion or exclusion of Feature SQA.

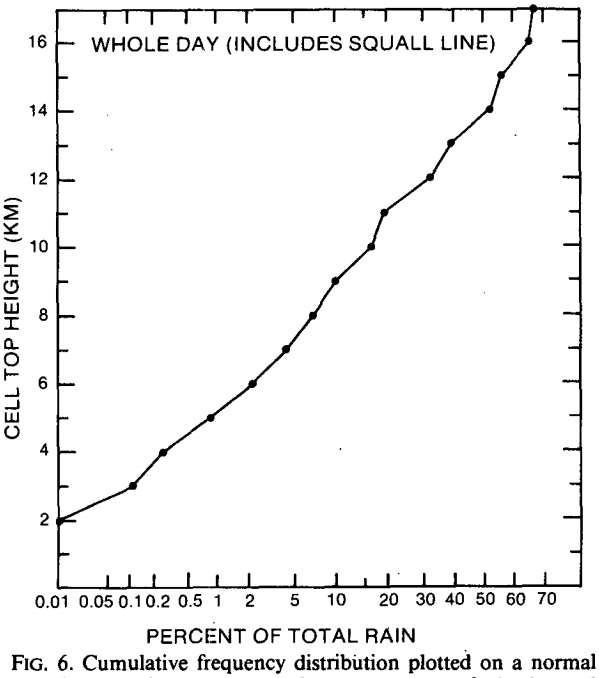

FIG. 6. Cumulative frequency distribution plotted on a normal probability scale of the percentage of the total amount of rain observed over the data collecting network in Fig. 1 during the interval 2300 4 September to 2400 5 September 1974 due to convective cells of different heights. Rainfall from all 12 precipitation features is included.

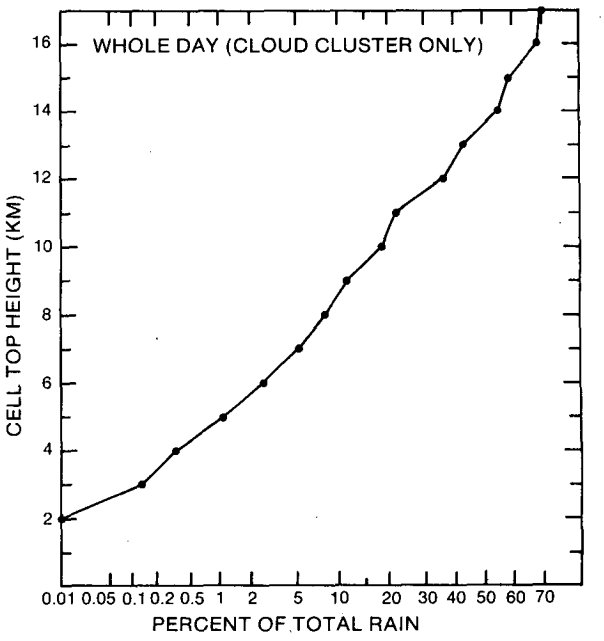

FIG. 7. As in Fig. 6, but with rain from Feature SQA excluded from the total amount of rain and the individual contributions from the convective cell top height categories.

b. Average rainfall rates associated with stratiform rain and convective cells of different height

Frequency distributions of the areas identified as being occupied by rain falling from cells of different heights and by stratiform rain are presented in Figs. 8 (all features) and 9 (Feature SQA excluded). In both distributions, the area covered by stratiform rain is quite extensive—in excess of 35% of the total number of squares reporting rainfall. Cells with tops below 10 km make a larger contribution to the frequency distributions of area than they do to the frequency distributions of rainfall. This is at least partly due to the 4 km × 4 km size of the squares. It would be extremely unlikely for the entire area of 16 km^2 to be occupied by cells in the shallower height categories, rather, the cells would be separated by rainfree areas. Also, rainfall rates are lower for the shallower cells.

Apart from emphasizing the importance of the area covered by stratiform rain, the frequency distributions in Figs. 8 and 9 are useful principally because they

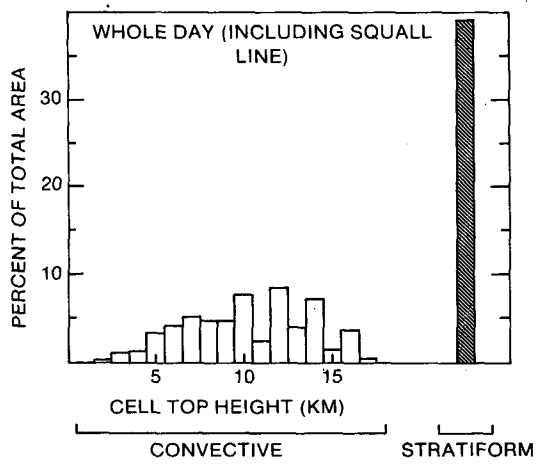

FIG. 8. As in Fig. 4, but for total area covered by precipitation, based on hourly subtotals of rainfall amounts, echo top heights and areas covered by precipitation over the data collecting network in Fig. 1.

provide the information, which, together with that contained in Figs. 5 and 6, can be used to calculate average rainfall rates. Since all raw rainfall amounts were hourly accumulations over areas of 16 km^2, rainfall rates were obtained by dividing the rainfall represented by each category in Figs. 5 and 6 by the corresponding areas represented by Figs. 8 and 9. Figs. 10 and 11 show the results of these computations.

The rainfall rates in Figs. 10 and 11 are about an order of magnitude lower than typical instantaneous precipitation rates associated with mesoscale precipitation systems. The apparent discrepancy is due to the hour-long period of averaging, the size of the data squares (16 km^2), which cannot be expected to be completely filled with precipitation, and the large number of such data squares that contributed to many of the 1008 subtotals. The rainfall rates in Figs. 10 and 11 are, however, suitable for comparison with and incorporation into satellite-derived estimates of rainfall because satellite data have a comparably coarse spatial and temporal resolution.

In both Figs. 10 and 11, the highest rainfall rates are associated with the deepest convective cells. The smooth progression to higher rainfall rates with deeper cells is broken only in the 12–13 km height range. This is probably due to two factors, the first of which is uncertainty in estimating echo tops. Second and perhaps more important, the 12–13 km layer marks the upper limit for all tops that do not overshoot the level of zero buoyancy (Cheng and Houze, 1979). Cells with tops of 14 km and higher are associated with especially high precipitation rates. These higher rainfall rates are consistent with either the presence of the more intense updrafts necessary to overshoot the level of zero buoyancy or a reduction of water load at a lower height than the shallower cells.

The average stratiform rainfall rates, 2.2 mm h^{-1} (including Feature SQA) and 2.0 mm h^{-1} (excluding Feature SQA) compare well with the values of 2.6 and 3.3 mm h^{-1} Gamache and Houze (1983) and Rappaport (1982) respectively, computed for the stratiform regions in the 12 September and 28 June GATE squall-line systems. The stratiform rainfall rates presented here also seem reasonable in comparison with the results of Zipser *et al.* (1981), although a quantitative

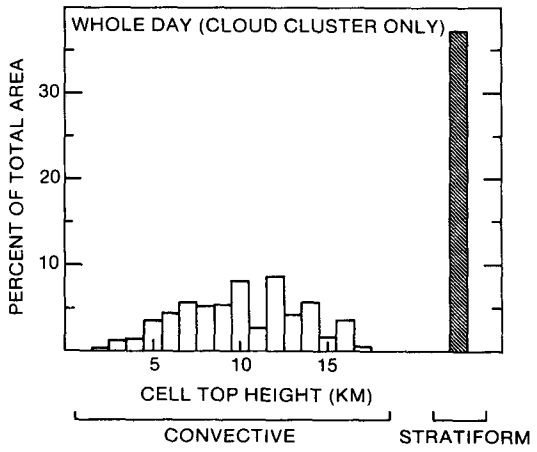

FIG. 9. As in Fig. 8, but with areas with precipitation from Feature SQA excluded from the total area and the individual contributions from the stratiform and convective cell top height categories.

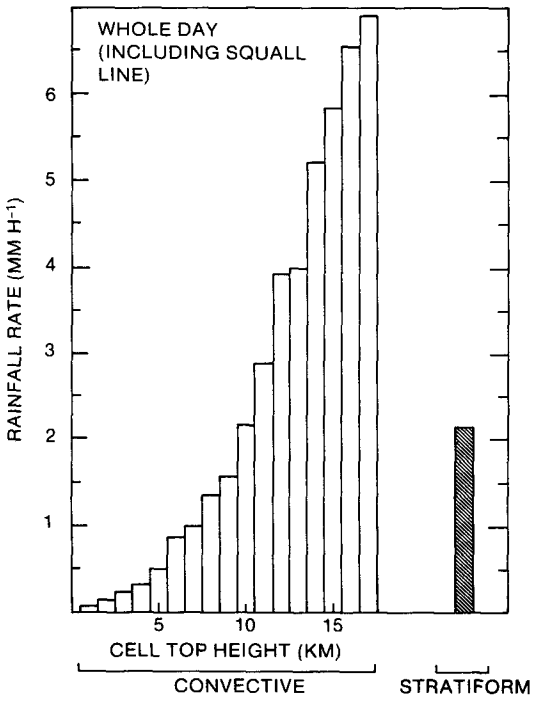

FIG. 10. Average rainfall rates for stratiform and convective cell top height categories computed by dividing the total rain in each category by the total area and time over which it fell. Rainfall from all 12 precipitation features is included.

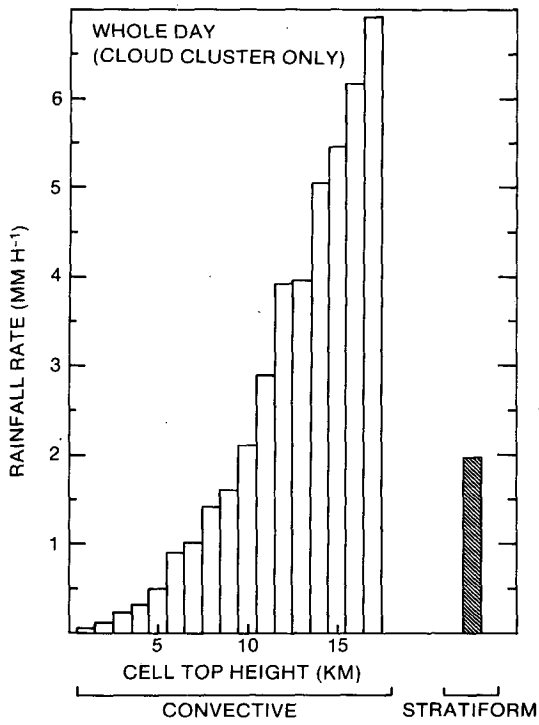

FIG. 11. As in Fig. 10, but rainfall from Feature SQA is not included.

comparison is not possible. Squall line systems apparently have somewhat more vigorous stratiform rainfall rates than do nonsquall features.

c. *Life cycle of the cloud cluster and the temporal distribution of precipitation over the data array*

Figure 12 illustrates the life cycle of the double cloud cluster of 5 September, excluding Feature SQA. Hourly rainfall amounts are plotted and labeled by the end of the hour for which they have been computed. The total precipitation, including both convective and stratiform precipitation, shows a definite life cycle, with a rather flat maximum in total rainfall from 0900 to 1900. Stratiform precipitation shows a considerable time lag. From 0000 to 0800 virtually all the rain was convective. Houze (1977), Houze and Rappaport (1984) and Churchill and Houze (1984) noticed a similar lag in the development of stratiform rain in the GATE squall-line systems of 4–5 September and 28 June and a nonsquall cloud cluster off the coast of Borneo respectively. Such time lags suggest that storage of condensate produced by convective cells may occur within the developing anvil cloud for several hours before falling out as stratiform rain along with water actually condensed within the anvil cloud.

Towards the end of the cloud cluster life cycle, convective and stratiform rain have comparable magnitudes. Overall, the precipitation life cycle of the cloud cluster is similar to that of the 4–5 September squall-line system computed by Houze (1977). This similarity is particularly interesting because the squall line system consisted of only one mesoscale precipitation feature, while the cloud cluster, which produced a comparable amount of total precipitation, consisted of at least four distinct mesoscale precipitation features. Thus, somewhat different modes of convective organization can, when viewed over their lifetimes on the larger mesoscale, produce similar precipitation statistics.

Both the 4–5 September squall-line system and the 5 September double cloud cluster were associated with the same synoptic-scale wave in the midtropospheric easterly flow (Houze, 1977; Leary, 1979). The squall line system formed and moved ahead of the trough of the easterly wave and the cloud cluster formed just ahead of and in the wave trough. Since the two systems account for virtually all of the rainfall associated with this easterly wave, rainfall data for both systems are combined in Fig. 13, where hourly precipitation amounts for the period 0800–2300 on 4 September were obtained by integrations from Fig. 26 of Houze

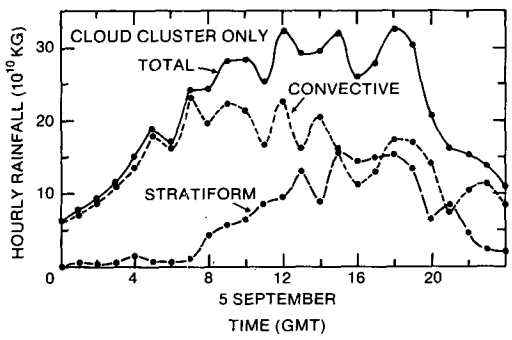

FIG. 12. Total, convective and stratiform hourly rainfall amounts observed over the data collecting network in Fig. 1 plotted as a function of time. Each data point includes precipitation for the preceding hour. Feature SQA has not been included in these precipitation amounts.

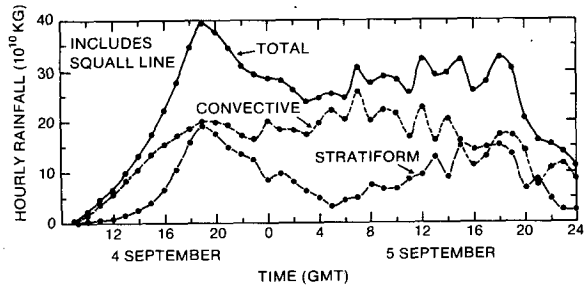

FIG. 13. Total, convective and stratiform hourly rainfall amounts observed over the data collecting network in Fig. 1 plotted as a function of time over the lifetime of the 4–5 September squall-line system and the 5 September double cloud cluster. Each data point includes precipitation for the preceding hour. For hours ending 0000–2400 on 5 September, the data are as presented in Fig. 12, with the addition of precipitation from Feature SQA. For earlier times, data points were obtained by hourly integrations from Fig. 26 of Houze (1977).

(1977) and hourly amounts from 2300 4 September to 2400 5 September are those of Fig. 9 with the addition of Feature SQA. The data from Houze (1977) are a slight underestimation of the total rain over the data network because his Fig. 26 included only rainfall associated with the squall line system. With the exception of the large peak at 1900 on 4 September, the total precipitation over the data network was relatively constant for nearly 24 hours. The convective precipitation amounts in Fig. 13 are also relatively constant over nearly a 24 h period. The stratiform rain, though, shows a broad minimum early on 5 September, when the squall line system was dissipating and moving out of radar range, and the cloud cluster had not yet developed significant amounts of stratiform rain. The two peaks in stratiform rain and the peak in total rain associated with the first of these are the only evidence in Fig. 13 to suggest that two different major precipitation systems, the second of which itself contained distinct mesoscale precipitation features, were responsible for the precipitation pattern associated with the trough region of the easterly wave.

d. Life cycles of mesoscale precipitation features in the cloud cluster

1) FEATURE E1

Of all the component features of the 5 September cloud cluster, Feature E1 had the most distinct life cycle and the fewest interactions with other features. Its distribution of total, convective and stratiform rainfall, shown in Fig. 14, has a strong similarity in shape to the overall rainfall pattern for the cloud cluster (Fig. 12), including a pronounced lag in the development of the stratiform rain in the early stages of its life cycle. Feature E1 was one of the principal precipitation features of 5 September (Fig. 3), contributing 19% of the total convective rain and 18% of the total stratiform rain.

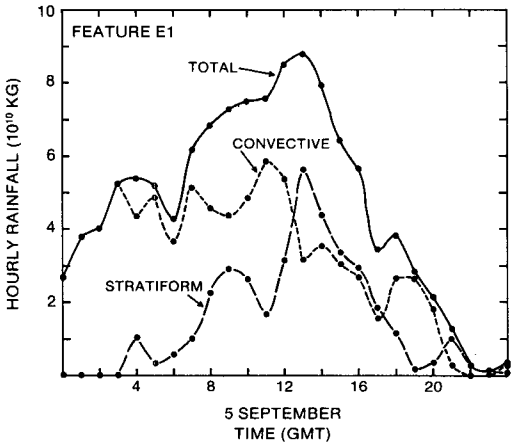

FIG. 14. Total, convective and stratiform hourly rainfall amounts for Feature E1 plotted as a function of time. Each data point includes precipitation for the preceding hour.

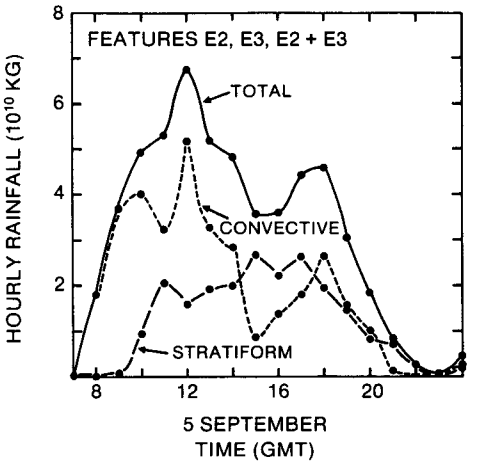

FIG. 15. As in Fig. 14, but for Features E2, E3 and E2 + E3. During the hour ending at 0700, all rain was convective.

2) FEATURES E2, E3 AND E2 + E3

The proximity of E2 and E3 and their common area of principally stratiform rain E2 + E3 (see Fig. 3), made it appropriate to combine their rainfall amounts in Fig. 15. Again, the pattern of total, convective and stratiform rain is similar to that of Feature E1 and the cloud cluster as a whole.

3) FEATURES N, M

Feature N's proximity to and association with Feature M suggested their combination in Fig. 16. While the overall pattern of total, convective and stratiform rain resembles Figs. 12, 14 and 15, the proportion of stratiform rain in Features N and M is considerably smaller. Together (see Fig. 3), they contribute only 4.2% of the total stratiform rain observed on 5 September. In light of the small absolute amount of strat-

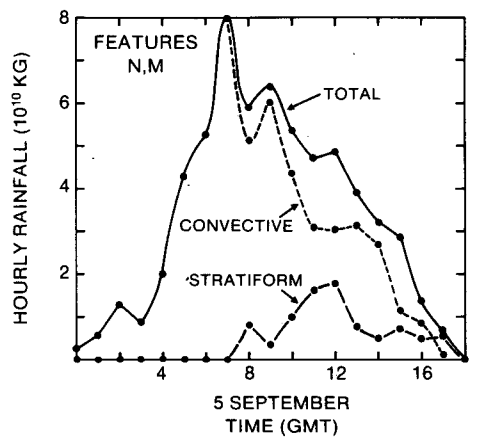

FIG. 16. As in Fig. 14, but for Features N and M. Prior to the hour ending at 0800, all rain was convective.

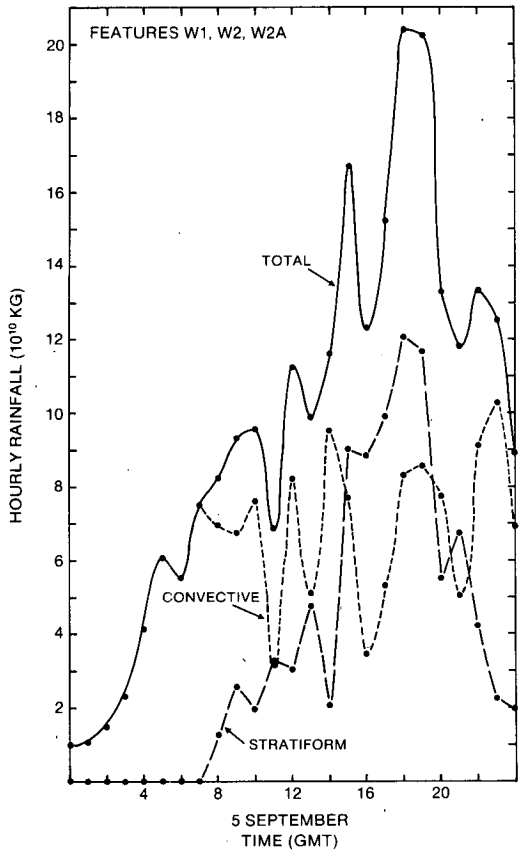

FIG. 17. As in Fig. 14, but for Features W1, W2 and W2A. Prior to the hour ending at 0800, all rain was convective.

iform rain, it is surprising that the general shape of Fig. 14 is so similar to that of features and combinations of features with much larger amounts of stratiform rain.

4) FEATURES W1, W2 AND W2A

Although Feature W1 formed before Features W2 and W2A, their interactions made separating their rainfall patterns difficult. When Feature W2 overtook Feature W1, some moisture condensed in convective cells in Feature W1 likely fell in the stratiform portions of Feature W2. Likewise, for some hours Feature W2A was difficult to distinguish from Feature W2. Fig. 17 shows the life cycle of precipitation from the combination of Features W1, W2 and W2A, which accounted for 38% of the total overall rainfall, 44% of the total stratiform rainfall and 35% of the total convective rainfall (see Fig. 3) on 5 September. The pattern is noisier than those for the other features and combinations of features, but shows the same general shape. The lag in the development of stratiform rain is quite distinct. Together, Figs. 14, 15, 16 and 17 include all of the rain associated with the double cloud cluster (Fig. 12) except Features SQB and L.

5. Conclusions

The precipitation statistics for the 5 September GATE double cloud cluster confirm the importance of deep convection and stratiform precipitation in tropical cloud clusters. During the period 2300 4 September to 2400 5 September, over an area of 42.5 $\times 10^4$ km^2 less than 10% of the total precipitation from the double cloud cluster fell from convective cells with echo top heights less than 9 km. Deeper convective cells accounted for more than 60% and stratiform precipitation accounted for 30% of the total precipitation. Average rainfall rates computed for convective cells of different heights from hourly rainfall totals in 4 km $\times$ 4 km data bins show that average rainfall rates increase with increasing echo top height.

The life cycles of the mesoscale precipitation features which made up the double cloud cluster of 5 September show similar precipitation structures. An important feature is a pronounced lag of three to seven hours in the development of the stratiform precipitation in the early stages of the life cycle, indicating the importance of the storage of condensate in the anvil cloud to the water budget of a mesoscale precipitation feature. When the life cycles of its constituent mesoscale features are superimposed, the evolution of the total, convective and stratiform amounts of rainfall in the 5 September double cloud cluster shows a strong similarity to comparable statistics for the mesoscale precipitation features of which it is composed, as well as to comparable statistics for squall line systems consisting of a single intense mesoscale precipitation feature. These similarities suggest that both mesoscale and synoptic-scale quantitative studies may, with confidence, use similar formulations to describe individual mesoscale precipitation features, their aggregate in a nonsquall tropical cloud cluster and the single very intense mesoscale precipitation feature which forms a tropical squall-line cloud cluster.

When precipitation from the 4–5 September squall-line system and the 5 September double cloud cluster are combined to show the evolution of precipitation over the large mesoscale in and near the trough of an easterly wave, the total rainfall is nearly constant for over 24 hours. This result is consistent with the statistical quasi-equilibrium assumption Arakawa and Schubert (1974) used to provide a closed parameterization of cumulus convection for use in prognostic models of large-scale atmospheric motion.

Acknowledgments. The original impetus for this research came from Prof. Robert A. Houze, Jr., at the University of Washington. Dr. Pauline M. Austin, Mr. Spiros Geotis and Dr. Frank Marks, all of the Department of Meteorology at the Massachusetts Institute of Technology, Dr. G. L. Austin of McGill University and Dr. Michael D. Hudlow of NOAA assisted this research by providing data and information about data collection and processing methods for the GATE radar

data. Mr. Edward N. Rappaport, Mrs. Sibani Chatterjee, Mr. Charles A. Clough, Mr. Jonathan C. Clough and Mr. Eric N. Clough all contributed to the processing of the data at Texas Tech University. Dr. John Gamache and Mr. Edward N. Rappaport performed some of the first data processing at the University of Washington. Ms. Susie Griffith drafted the figures and Ms. Denise Bentley typed the manuscript. Dr. Margaret A. LeMone of the National Center for Atmospheric Research and Prof. Robert A. Houze, Jr. read the manuscript and made many useful comments.

This research was supported by the National Science Foundation under Grant ATM-8006100. The earliest phases of the work were performed when the author was affiliated with the University of Washington and supported by the National Science Foundation under Grant ATM-7414830 (Principal Investigator: Prof. Robert A. Houze, Jr.). From 1 September 1979 to 31 August 1980, this research was supported by a state-organized research grant sponsored by the College of Arts and Sciences at Texas Tech University.

REFERENCES

Arakawa, A., and W. H. Schubert, 1974: Interaction of a cumulus cloud ensemble with the large-scale environment, Part I. *J. Atmos. Sci.*, **31,** 674–701.

Austin, G. L., 1977a: Documentation for GATE *Quadra* radar digital PPI data. *GATE Processed and Validated Data,* 27 pp. [see EDS, 1975].

——, 1977b: Documentation for radar, *Quadra* microfilm data set. *GATE Processed and Validated Data,* 3 pp. [see EDS, 1975]

Austin, P. M., 1976a: Documentation for Gilliss radar Cartesian hybrid data set. *GATE Processed and Validated Data,* 79 pp. [see EDS, 1975]

——, 1976b: Documentation for Gilliss radar images on 35 mm film. *GATE Processed and Validated Data,* 65–74. [see EDS, 1975]

——, 1976c: Documentation for Gilliss radar raw digital data. *GATE Processed and Validated Data,* 50 pp. [see EDS, 1975]

Cheng, C.-P., and R. A. Houze, Jr., 1979: The distribution of convective and mesoscale precipitation in GATE radar echo patterns. *Mon. Wea. Rev.*, **107,** 1370–1381.

Churchill, D. D., and R. A. Houze, Jr., 1984: Development and structure of winter monsoon cloud clusters on 10 December 1978. *J. Atmos. Sci.*, **41** (in press).

EDS, 1975: *GATE Data Catalogue.* [Available from GATE World Data Center-A, National Climate Center, Environmental Data Service (EDS), NOAA, Federal Building, Asheville, NC.]

Gamache, J. F., and R. A. Houze, Jr., 1983: Water budget of a mesoscale convective system in the tropics. *J. Atmos. Sci.*, **40,** 1835–1850.

Hamilton, R. A., and J. W. Archbold, 1945: Meteorology of Nigeria and adjacent territory. *Quart. J. Roy. Meteor. Soc.*, **71,** 231–264.

Houze, R. A., Jr., 1977: Structure and dynamics of a tropical squall-line system. *Mon. Wea. Rev.*, **105,** 1540–1567.

——, 1981: Structures of atmospheric precipitation systems: A global survey. *Radio Sci.*, **16,** 671–689.

——, and C.-P. Cheng, 1977: Radar characteristics of tropical convection observed during GATE: Mean properties and trends over the summer season. *Mon. Wea. Rev.*, **105,** 964–980.

——, and A. K. Betts, 1981: Convection in GATE. *Rev. Geophys. Space Phys.*, **16,** 541–576.

——, and E. N. Rappaport, 1984: Air motions and precipitation structure of an early summer squall line over the eastern tropical Atlantic. *J. Atmos. Sci.*, **41,** 553–574.

Hudlow, M. D., 1975a: Documentation for GATE *Oceanographer* radar film. *GATE Processed and Validated Data,* 50 pp. [see EDS, 1975]

——, 1975b: Documentation for GATE raw digital data subset. *GATE Processed and Validated Data,* 61 pp. [see EDS, 1975]

——, 1976a: Documentation for GATE NOAA hybrid microfilm graphics data. *GATE Processed and Validated Data,* 12 pp. [see EDS, 1975]

——, 1976b: Documentation for GATE NOAA hybrid data. *GATE Processed and Validated Data,* 18 pp. [see EDS, 1975]

——, 1976c: Documentation for *Researcher* radar images on 35 mm microfilm. *GATE Processed and Validated Data,* 18 pp. [see EDS, 1975]

——, 1977: Hourly radar precipitation data. *GATE Processed and Validated Data,* 15 pp. [see EDS, 1975]

——, 1979: Mean rainfall patterns for the three phases of GATE. *J. Appl. Meteor.*, **18,** 1656–1669.

——, and V. L. Patterson, 1979: *GATE Radar Rainfall Atlas.* NOAA Spec. Rep., Center for Environmental Assessment Services, NOAA, 155 pp. [Govt. Printing Office Stock No. 003-019-00046-2].

——, R. Arkell, V. Patterson, P. Pytlowany, F. Richards and S. Geotis, 1979: Calibration and intercomparison of the GATE C-band weather radars. NOAA Tech. Rep. EDIS 31, Center for Environmental Assessment Services, NOAA, 98 pp.

Leary, C. A., 1979: Behavior of the wind field in the vicinity of a cloud cluster in the Intertropical Convergence Zone. *J. Atmos. Sci.*, **36,** 631–639.

——, and R. A. Houze, Jr., 1979a: The structure and evolution of convection in a tropical cloud cluster. *J. Atmos. Sci.*, **36,** 437–457.

——, and ——, 1979b: Melting and evaporation of hydrometeors in precipitation from the anvil clouds of deep tropical convection. *J. Atmos. Sci.*, **36,** 669–679.

Payne, S. W., and M. M. McGarry, 1977: The relationship of satellite inferred convective activity to easterly waves over West Africa and the adjacent ocean during Phase III of GATE. *Mon. Wea. Rev.*, **105,** 413–420.

Rappaport, E. N., 1982: Structure and dynamics of an atypical tropical squall-line system. M.S. thesis, University of Washington, Seattle, 266 pp.

Riehl, H., and J. S. Malkus, 1958: On the heat balance in the equatorial trough zone. *Geophysica,* **6,** 503–538.

Zipser, E. J., 1969: The role of organized unsaturated convective downdrafts in the structure and rapid decay of an equatorial disturbance. *J. Appl. Meteor.*, **8,** 799–814.

——, R. J. Meitín and M. A. LeMone, 1981: Mesoscale motion fields associated with a slowly moving GATE convective band. *J. Atmos. Sci.*, **38,** 1725–1750.